Eur. Phys. J. A **15**, 27–33 (2002)
DOI 10.1140/epja/i2001-10219-7

THE EUROPEAN PHYSICAL JOURNAL A

Nuclear-matter distributions of halo nuclei from elastic proton scattering in inverse kinematics

P. Egelhof[1,a], G.D. Alkhazov[2], M.N. Andronenko[2], A. Bauchet[1], A.V. Dobrovolsky[1,2], S. Fritz[1], G.E. Gavrilov[2], H. Geissel[1], C. Gross[1], A.V. Khanzadeev[2], G.A. Korolev[2], G. Kraus[1], A.A. Lobodenko[2], G. Münzenberg[1], M. Mutterer[3], S.R. Neumaier[1], T. Schäfer[1], C. Scheidenberger[1], D.M. Seliverstov[2], N.A. Timofeev[2], A.A. Vorobyov[2], and V.I. Yatsoura[2]

[1] Gesellschaft für Schwerionenforschung (GSI), D-64291 Darmstadt, Germany
[2] Petersburg Nuclear Physics Institute (PNPI), RU-188300 Gatchina, Russia
[3] Institut für Kernphysik (IKP), Technische Universität, D-64289 Darmstadt, Germany

Received: 21 March 2002 /
Published online: 31 October 2002 –

Abstract. Proton-nucleus elastic scattering at intermediate energies, a well-established method for probing nuclear-matter density distributions of stable nuclei, was applied for the first time to exotic nuclei. This method is demonstrated to be an effective means for obtaining accurate and detailed information on the size and radial shape of halo nuclei. Absolute differential cross-sections for small-angle scattering were measured at energies near 700 MeV/u for the neutron-rich helium isotopes ^{6}He and ^{8}He, and more recently for the lithium isotopes ^{6}Li, ^{8}Li, ^{9}Li and ^{11}Li, using He and Li beams provided by the fragment separator FRS at GSI Darmstadt. Experiments were performed in inverse kinematics using the hydrogen-filled ionization chamber IKAR which served simultaneously as target and recoil-proton detector. For deducing nuclear-matter distributions, differential cross-sections calculated with the aid of the Glauber multiple-scattering theory, using various parametrizations for the nucleon density distributions as input, were fitted to the experimental cross-sections. The results on nuclear-matter radii and matter distributions are presented, and the significance of the data for a halo structure is discussed. Nuclear-matter distributions obtained for ^{6}He and ^{8}He conform with the concept that both nuclei compose of α-particle like cores and significant neutron halos. The matter distribution in ^{11}Li exhibits, as expected from previous reaction cross-section studies with nuclear targets, the by far most extended halo component of all nuclei being investigated. In addition the present data allow a quantitative comparison of the structure of the He and Li isobares of either the mass number $A = 6$ or $A = 8$. The measured differential cross-sections have also been used for probing density distributions as predicted from various microscopic calculations. A few examples are presented.

PACS. 21.10.Gv Mass and neutron distributions – 25.40.Cm Elastic proton scattering – 27.20.+n $5 \leq A \leq 19$

1 Introduction

The size of nuclei and the radial shape of the distribution of nuclear matter and charge are fundamental properties of nuclei, and therefore of high interest for various fields in nuclear physics. Accurate experimental data on the moments of the charge and matter distributions are of particular interest for the understanding of nuclear structure and for probing theoretical model descriptions of nuclei. Over the years a large variety of experimental methods were developed, using leptonic probes (as electrons, muons, etc.) for investigating nuclear charge distributions, and hadronic probes (as protons, α-particles, pions, etc.) for exploring the distributions of nuclear matter (see ref. [1] for an overview). While all these methods were applied successfully for many years for the study of stable nuclei, the investigation of the size and radial shape of exotic nuclei has become a new and exciting field of research.

One of the outstanding results in nuclear physics with exotic beams was the discovery that the nuclear matter may appear under certain conditions with a qualitatively new type of nuclear structure, the so-called "halo" structure. Compared to the stable nuclei and those close to stability, in which all the protons and neutrons are essentially distributed uniformly over the nuclear volume, and the nuclear r.m.s. radius R_m scales approximately with mass number A (by $R_\mathrm{m}(A) = r_0 A^{1/3}$), it was found that some

[a] e-mail: p.egelhof@gsi.de

light neutron-rich nuclei located at or near the neutron drip line exhibit a far extended low-density distribution of loosely bound valence neutrons (the "halo") surrounding a compact distribution of the majority of nucleons (the "core"). The discovery of this phenomenon and its interpretation in terms of the halo picture was initiated by the pioneering work of Tanihata *et al.* [2], where total cross-sections σ_{I} were determined for the interaction of light neutron-rich isotopes with various targets. The surprisingly steep rise of σ_{I} for ^{11}Li in the sequence of the Li isotopes and also, but less pronounced, for the He isotopes ^{6}He and ^{8}He, was interpreted as being due to a pronounced increase of the nuclear-matter radius. Later a similar behavior was found for a couple of other isotopic chains [2]. In order to get deeper insight into the structure of neutron-rich nuclei, the halo phenomenon has been the subject of numerous studies during the last decade (see [3–8] for an overview). Various experimental methods were applied, such as beta-decay measurements following in-beam polarization by optical pumping, and the investigation of momentum distributions of the reaction products after fragmentation of halo nuclei following interaction with target nuclei. The picture of nuclear halo structure established soon after the observation of the large interaction radii was qualitatively confirmed. Halo nuclei are thus assumed to be composed of a nuclear core and a number (one, two or four) of valence neutrons, and are characterized, besides the large interaction cross-sections, by similar electric and magnetic moments of the halo nuclei and the nuclei corresponding to their cores, weak binding energies of the valence nucleon(s), and narrow momentum distributions of the reaction products following fragmentation.

Nevertheless, it should be pointed out, that probing the radial structure and size of halo nuclei with experiments on total reaction cross-sections and momentum distributions of the fragments is considerably limited by the incomplete knowledge of the rather complicated mechanisms and dynamics of the reactions involved. Hence, systematic errors in the determination of matter radii are likely to appear [8]. Therefore, accurate and detailed information on the matter radii and on the radial shapes of halo nuclei is desirable from other sources. The present contribution deals with the application of a (for the investigation of exotic nuclei) new and independent method, *i.e.* elastic proton scattering at intermediate energies.

2 Intermediate-energy elastic proton scattering —a tool to study the structure of halo nuclei

Proton-nucleus elastic scattering at intermediate energies around 700–1000 MeV is known to be a method well established for obtaining accurate nuclear-matter distributions in stable nuclei [1,9]. This method was applied at GSI Darmstadt for the first time for the investigation of exotic nuclei by using the technique of inverse kinematics. The advantage of choosing protons at intermediate energies as probes is mainly due to the capability

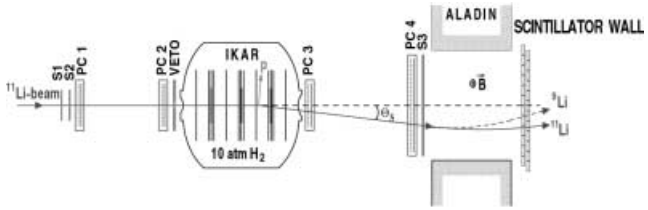

Fig. 1. Schematic view of the experimental setup for small-angle elastic proton scattering on exotic nuclei in inverse kinematics. The central part shows the hydrogen-filled ionization chamber IKAR which serves simultaneously as a gas target and detector for recoil protons. The forward spectrometer (multi-wire proportional chambers PC1-PC4) determines the scattering angle θ_{S} of the projectile. Scintillation counters (S1-S3, VETO) and the ALADIN magnet are used for beam identification and background discrimination.

of the Glauber multiple-scattering theory of accurately describing the scattering process in this energy region, which, by using as input the proton-nucleon amplitudes from free proton-nucleon scattering data, permits to correlate the differential elastic-scattering cross-sections and the matter distributions of the composite nuclei in an unambiguous way [9]. On the contrary, from data taken at lower energies around E = 20–100 MeV (see for example [10–13]) a quantitative determination of the moments of the nuclear-matter distribution is considerably limited, or even impossible, due to potential ambiguities and (or) uncertainties in the effective proton-nucleon amplitudes, which are much better known at intermediate energies. For the case of intermediate incident energies, simulation calculations performed for pHe and pLi scattering [14,15] have clearly demonstrated that proton scattering in the region of small momentum transfer is particularly sensitive to the nuclear-matter radius, and the halo structure of nuclei. It turns out, that the slope of the differential cross-section is directly correlated with the nuclear-matter radius R_{m}, whereas its curvature contains information on the radial shape of the halo structure. Thus, besides determining precisely the nuclear-matter radius, the shape of the nuclear-matter distribution in halo nuclei can be explored already from data in the limited range of momentum transfer at small scattering angles.

Differential cross-sections for elastic proton scattering at small momentum transfer were measured at GSI Darmstadt at energies around 700 MeV/u in inverse kinematics for the neutron-rich helium isotopes ^{6}He, ^{8}He [16,17], and more recently for the neutron-rich lithium isotopes ^{8}Li, ^{9}Li, and ^{11}Li. Additionally, data were taken for the stable isotopes ^{4}He and ^{6}Li for providing a consistency check of the method applied. The secondary He and Li beams were produced by fragmentation of ^{18}O ions from the heavy-ion synchrotron SIS impinging on a beryllium target, and were isotopically separated by the fragment separator FRS. Beam intensities were of the order of $10^3\,\mathrm{s}^{-1}$ in all cases.

The experimental setup is displayed in fig. 1. The relatively low secondary beam intensities for isotopes close to the drip line demand for a thick effective hydrogen tar-

get, and for a large-solid-angle detector for the recoil protons. In order to meet these conditions, the hydrogen-filled multiple-ionization chamber IKAR was used, which serves simultaneously as target and detector. IKAR ensures a high H_2 target thickness (about 3×10^{22} protons/cm^2), and has a 2π acceptance in azimuthal angle for recoil-proton registration. It operates at 10 bar hydrogen pressure and consists of 6 identical modules. Each module contains an anode plate, a cathode plate, and a grid, all electrodes being arranged perpendicularly to the beam direction. The signals from the electrodes, registered by flash analog-to-digital converters, provide the energy of the recoil proton, or its energy loss in case it leaves the active volume, the scattering angle of the recoil proton, and the vertex point. The scattering angle θ_S for the helium (lithium) projectiles was determined by a tracking detector consisting of 4 two-dimensional multiwire-proportional chambers (PC1-4). In addition, scintillation counters S1, S2, S3, and VETO were used for triggering, and for identification of incident and scattered beam particles via time-of-flight and dE/dx measurements. Furthermore, a magnetic-rigidity analysis of the scattered projectiles was performed in part of the Li measurements with the aid of the ALADIN magnet and a position-sensitive scintillator wall behind, for the discrimination from projectile break-up channels.

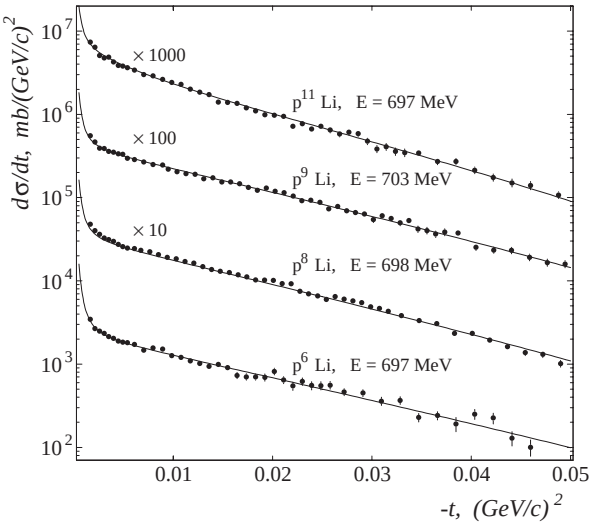

Fig. 2. Differential cross-sections $d\sigma/dt$ *versus* the four-momentum transfer squared t for p^{6,8,9,11}Li elastic scattering (preliminary data). Energies are the equivalent proton energies for normal kinematics. Lines are the result of fits to the data performed on the basis of the Glauber multiple scattering theory (for details see text).

3 Results on nuclear-matter density distributions and matter radii of neutron-rich He and Li isotopes

The differential cross-sections deduced from the present experiment for the Li isotopes investigated are displayed in fig. 2 *versus* the four-momentum transfer squared t. Data of similar quality have been obtained for the ^{4,6,8}He isotopes (see refs. [16–18] and fig. 5 below). It should be noted that all data on the Li isotopes presented here are still preliminary. For establishing the nuclear density distributions from the measured cross-sections, the Glauber multiple scattering theory was applied. Calculations were performed using the basic Glauber formalism [9] for proton-nucleus elastic scattering, and taking experimental data on the elementary proton-proton and proton-neutron scattering amplitudes as input. For modeling the nuclear-matter density distribution, various parametrical functions were used, each of them having two free parameters to allow for reproducing an extended matter distribution as expected for halo nuclei (for details see refs. [14,16]). The free parameters of the density distribution parametrizations were determined by a least-square fit of the calculated cross-sections to the experimental ones. Conventionally all matter distributions $\rho_m(r)$ deduced, as well as the resulting matter radii R_m, refer to the point nucleon density. As a result of the fitting procedure the measured cross-sections for all isotopes investigated are well described, independent of the parametrization used, with reduced χ^2-values around unity in all cases. The solid lines displayed in fig. 2 represent the results for one parametrization (GG, see below) as an example. Concerning the results on the size and radial shape of the nuclear-matter distributions, it was already demonstrated for the ^{4,6,8}He isotopes [14,16], and more recently for the ^{6,8,9,11}Li isotopes [18], that the matter distributions as well as the corresponding matter radii deduced for the various parametrizations mutually agree within small errors. This demonstrates that the present results are quite independent of the choice of the parametrization. Within the frame of the present contribution the discussion will be restricted to only two selected parametrizations of the density distribution. They consist of a Gaussian distribution for the core nucleons, and either a Gaussian (GG) or a $1p$-shell harmonic oscillator-type density (GO) for the valence neutrons (for details see [14,16]). Both parametrizations applied allow to deduce, besides the total nuclear-matter distribution, also information on the distribution of the core and of the halo nucleons. For this purpose the halo nuclei were assumed to consist of an α-particle like core and 2 (4) valence neutrons in ^{6}He (^{8}He), and a ^{9}Li-like core and 2 valence neutrons in ^{11}Li.

The present results on the nuclear-matter distributions and matter radii of the Li and He isotopes are displayed in figs. 3-5 and table 1. Concerning the stable isotopes ^{4}He and ^{6}Li, where neutrons and protons are expected to be equally distributed, the nuclear-matter distributions deduced can be compared with the nuclear charge distributions resulting from electron scattering data [19]. A remarkably good agreement is obtained for both cases (see fig. 3 and refs. [14,16]) which may be interpreted as a successful consistency check of the present experimental method, including the procedure applied for the data analysis.

Table 1. A summary of nuclear-matter radii (average values resulting from various parametrizations applied) deduced for the helium isotopes ^{4,6,8}He and for the lithium isotopes ^{6,8,9,11}Li from the present experiment is given on the left side of the table. $R_{\rm m}$ denotes the total rms matter radius, $R_{\rm c}$ the core radius, and $R_{\rm h}$ the halo radius. The errors include statistical and systematical uncertainties. The results on $R_{\rm m}$ are compared to total nuclear matter radii deduced from data on total interaction cross-sections $\sigma_{\rm I}$ [2] obtained from an analysis of Tanihata *et al.* [20,21] and from a more recent re-analysis [22,23] of the same data.

	Results of present experiment			Results from $\sigma_{\rm I}$	
Nucleus	$R_{\rm c}$ (fm)	$R_{\rm h}$ (fm)	$R_{\rm m}$ (fm)	$R_{\rm m}$ (fm) [20,21]	$R_{\rm m}$ (fm) [22,23]
^{4}He	–	–	1.49 (3)	–	–
^{6}He	1.88 (12)	2.97 (26)	2.30 (7)	2.33 (4)	2.54 (4)
^{8}He	1.55 (15)	3.08 (10)	2.45 (7)	2.49 (4)	–
^{6}Li	2.08 (18)	3.04 (45)	2.45 (7)	2.32 (3)	–
^{8}Li	–	–	2.45 (6)	2.37 (2)	–
^{9}Li	–	–	2.43 (7)	2.32 (2)	2.30 (2)
^{11}Li	2.55 (12)	6.54 (38)	3.62 (19)	3.12 (16)	3.53 (10)

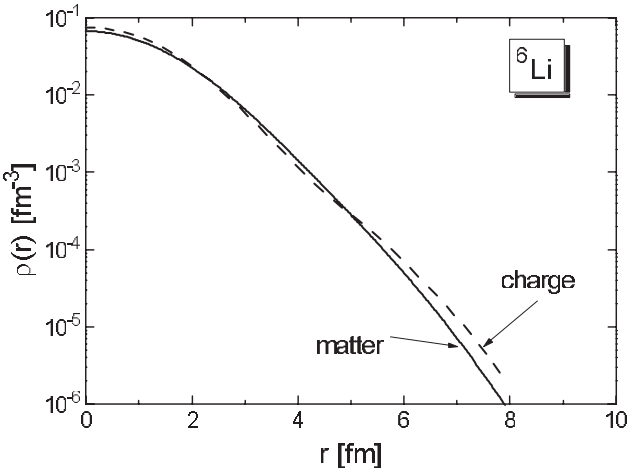

Fig. 3. The nuclear-matter distribution for ^{6}Li (solid line), deduced from the present experiment, is compared with the nuclear charge distribution of ^{6}Li (dashed line), deduced from data on electron scattering [19]. To allow a direct comparison the point matter density is folded with the nucleon size. The corresponding radii $R_{\rm m}$ (folded) = 2.58 (7) fm and $R_{\rm charge}$ = 2.56 (5) fm are in excellent agreement.

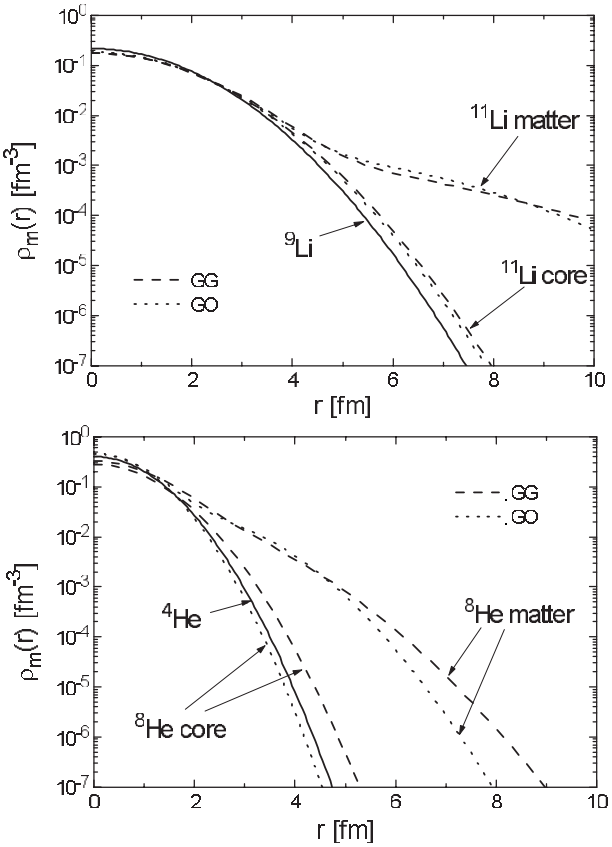

Fig. 4. Top: the nuclear-matter and nuclear core density distributions of ^{11}Li, deduced by using the GG and GO parametrizations (see text), are compared with the nuclear-matter density distribution obtained for ^{9}Li. Bottom: corresponding results on the matter and core distributions for ^{8}He and the matter distribution for ^{4}He.

The radial distributions of total nuclear matter and core matter, deduced from the present data, are displayed in fig. 4 for the halo nuclei ^{11}Li and ^{8}He together with the deduced matter distributions for the ^{9}Li and ^{4}He nuclei, supposed to be the respective cores. Obviously the results on the matter and core distributions obtained with the two parametrizations GG and GO are in reasonably good agreement with each other. Rather extended matter distributions are obtained for ^{11}Li and ^{8}He, as well as for ^{6}He (see fig. 5 and ref. [16]), the matter densities decreasing much slower with the radius parameter than the ones for ^{9}Li and ^{4}He, respectively. The results represent clear evidence for significant neutron halos in ^{11}Li and ^{6,8}He. The direct comparison of the results on ^{11}Li and ^{6,8}He (see figs. 4, 5) shows that ^{11}Li exhibits the by far most pronounced halo structure from all the nuclei at hand. This is also reflected in the deduced nuclear-matter radius $R_{\rm m}$ = 3.62 (14) fm and the halo radius $R_{\rm h}$ = 6.54 (38) fm, the latter being more than twice as large as in ^{6}He and ^{8}He (see table 1). The close resemblance of the core distributions in ^{11}Li and ^{6,8}He with the matter distributions of the ^{9}Li and ^{4}He nuclei (see fig. 4 for ^{11}Li

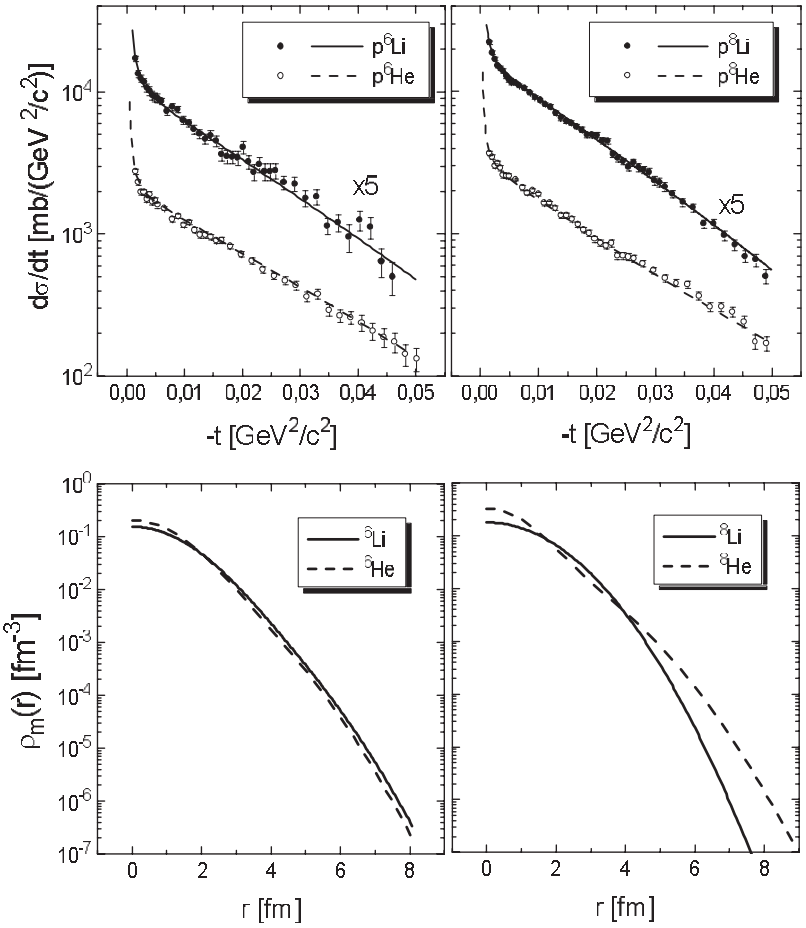

Fig. 5. Measured differential cross-sections $d\sigma/dt$ (top) and the deduced nuclear-matter density distributions $\rho_m(r)$ (bottom) are compared for the $A = 6$ isobares ^{6}Li and ^{6}He, and for the $A = 8$ isobares ^{8}Li and ^{8}He.

and ^{8}He, and ref. [15] for ^{6}He), supports the generally accepted picture of a two-neutron halo structure in ^{11}Li and ^{6}He, and a four-neutron halo structure in ^{8}He. The corresponding radii R_c of the cores are in all cases slightly larger than the nuclei supposed to be the respective cores (see table 1). This behaviour is explained as originating from the common motion of the core nucleons around the center of mass of the whole nucleus, which somewhat increases the effective core size.

The present systematic study of the He and Li isotopic chains with the same experimental method permits also for a direct comparison of the structure of either the $A = 6$ and $A = 8$ isobares. The cross-sections and the nuclear-matter distributions deduced for the ^{6}He, ^{6}Li and ^{8}He, ^{8}Li isotopes are displayed in fig. 5. Note that the measured ^{6}Li cross-section exhibits a significantly steeper slope than the one for ^{6}He, indicating the ^{6}Li radius to be larger than the ^{6}He radius. Consequently the matter distribution deduced for ^{6}Li is slightly more extended than the one for ^{6}He, which is also reflected in the matter radii obtained (see table 1). On the other hand, the close resemblance of the shapes of the matter distributions of ^{6}He and ^{6}Li may indicate that ^{6}Li features in fact also a halo structure with an α-like core and a deuterium cluster forming kind of a halo. The situation is quite different for the comparison of the ^{8}Li and ^{8}He nuclei. While both nuclei have essentially the same radius, their radial matter distributions are significantly different. Compared to the clear halo structure in ^{8}He, the matter distribution in ^{8}Li is significantly less extended, and can be approximated by a Gaussian shape. Accordingly, the t-dependence of the measured ^{8}Li cross-section is close to an exponential function, whereas the ^{8}He cross-section exceeds an exponential shape at the higher momentum transfers. The latter behaviour is a characteristic token for a halo structure [14,15].

The present results on nuclear-matter radii R_m from elastic proton scattering cross-sections may also be compared to corresponding data deduced from total interaction cross-sections (see table 1). Such a comparison is of special interest, as both methods of determining nuclear-matter radii are independent of each other. For the ^{6,8}He isotopes the results from the present experiment are in close agreement with the values deduced from Tanihata *et al.* [20]. However, the values on the matter radii deduced from total interaction cross-sections measured by Tanihata *et al.* [2] became recently in dispute, as a reanalysis [22,23] of the same data resulted in different values for R_m. So the most recent value [23] given for ^{6}He is larger than the result of the present experiment (see ref. [14] for a more detailed discussion). As for the matter

radii of the Li isotopes the situation is different. The results on ^{6}Li, ^{8}Li and ^{9}Li from the present experiment are slightly larger than the values from Tanihata *et al.* [21], and —for ^{9}Li— from a re-analysis of the same data by Al-Khalili *et al.* [22]. For ^{11}Li, the result from the present experiment also exceeds the value $R_{\rm m} = 3.12$ (16) fm from Tanihata *et al.* [21], but is in close agreement with the value from a re-analysis of the same data performed by Al-Khalili *et al.* [22]. Within errors the present result for ^{11}Li is consistent with the value $R_{\rm m} = 3.28$ (24) fm deduced from data on the (π^-, π^+) reaction [24].

Besides the determination of nucleon density distributions and their parameters, the present cross-section data also allow a sensitive test of theoretical model calculations on the structure of neutron-rich nuclei. For this purpose, the nucleon density distributions obtained from theoretical calculations were used as an input for Glauber calculations. The resulting "theoretical cross-sections" were compared with the experimental data. A systematic comparison of various theoretical results for ^{6,8}He, and most recently also for ^{11}Li, with the present data can be found in [8,14,15]. As an example the results of theoretical calculations for ^{11}Li, using the refined resonating group model [25] (line 1 in fig. 6), the dynamic correlation model [26] (line 2), a few-body Faddeev approach [27] with two different wave functions (lines 3 and 4), and a Hartree-Fock-Bogolubov approach [28] (line 5) are displayed in fig. 6 in comparison with the cross-section data from the present experiment. From the χ^2-values obtained it follows that the wave function "P4" from Thompson *et al.* [27] and the result from Lenske *et al.* [28] yield the best agreement with the experimental data. Generally it is concluded that the cross-section data from elastic proton scattering allow a selective test of theoretical model calculations, as they bear significantly more information on the details of nuclear structure, than a single number does, *i.e.* the nuclear-matter radius $R_{\rm m}$, commonly used for a comparison.

In summary the present work has demonstrated that small-angle elastic proton scattering at intermediate energies is a powerful tool for studying the structure of exotic light nuclei. In particular, the cross-section data obtained in inverse kinematics have allowed an accurate determination of the size and radial shape of the nuclear-matter distributions for a series of He and Li isotopes and have provided a clear evidence for a rather extended nuclear-matter distribution in ^{11}Li, and less pronounced ones in ^{6}He and ^{8}He.

For the future the present method is planned to be extended to heavier neutron- and proton-rich halo candidates, such as ^{14}B and ^{8}B, etc. and, for the nuclei already investigated, to the region of higher momentum transfer. In a very recent experiment the present data for p^{4,6,8}He scattering have already been extended to substantially higher momentum transfer, using a similar experimental technique, but replacing the active hydrogen gas target IKAR by a liquid-hydrogen target [29]. The data, presently being analyzed, are expected to allow a more detailed insight into the internal structure of halo nuclei, such as the structure of the core, and space correlations between the halo neutrons.

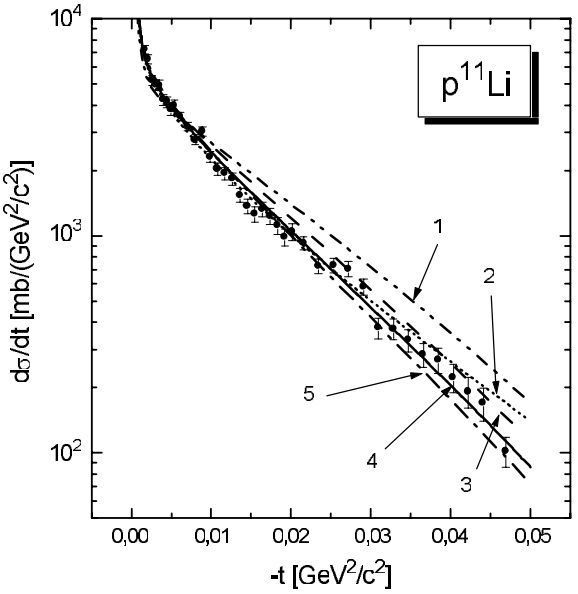

Fig. 6. Differential cross-sections for p^{11}Li scattering obtained from the present experiment (dots) are compared with calculated cross-sections on the basis of nuclear-matter distributions resulting from theoretical model calculations. The lines (1-5) correspond to the theoretical nuclear-matter densities from [25, 26], and [27] (for two different wave functions "P0" and "P4"), and from [28] (for details see text).

References

1. J.W. Negele *et al.*, Adv. Nucl. Phys. **19**, 1 (1989).
2. I. Tanihata *et al.*, Phys. Rev. Lett. **55**, 2676 (1985); Phys. Lett. B **160**, 380 (1985); Nucl. Phys. A **488**, 113c (1988).
3. K. Riisager, Rev. Mod. Phys. **66**, 1105 (1994).
4. P.G. Hansen *et al.*, Annu. Rev. Nucl. Part. Sci. **45**, 591 (1995).
5. I. Tanihata, Prog. Part. Nucl. Phys. **35**, 505 (1995).
6. I. Tanihata, J. Phys. G **22**, 157 (1996).
7. B. Johnson *et al.*, Philos. Trans. R. Soc. London, Ser. A **358**, 2063 (1998).
8. P. Egelhof, Acta Phys. Pol. B **30**, 487 (1999) and references therein.
9. G.D. Alkhazov *et al.*, Phys. Rep. C **42**, 89 (1978).
10. A. Korsheninikov *et al.*, Nucl. Phys. A **617**, 45 (1997).
11. D. Cortina-Gil *et al.*, Phys. Lett. B **401**, 9 (1997).
12. R. Wolski *et al.*, Phys. Lett. B **467**, 8 (1999).
13. A. Lagoyannis *et al.*, Phys. Lett. B **518**, 27 (2001).
14. G.D. Alkhazov *et al.*, to be published in Nucl. Phys. A (2002).
15. P. Egelhof *et al.*, Prog. Part. Nucl. Phys. **46**, 307 (2001).
16. G.D. Alkhazov *et al.*, Phys. Rev. Lett. **78**, 2313 (1997).
17. S.R. Neumaier *et al.*, to be published in Nucl. Phys. A (2002).
18. A. Dobrovolsky *et al.*, in preparation.
19. G.C. Li *et al.*, Nucl. Phys. A **162**, 583 (1971); H. de Vries *et al.*, At. Data Nucl. Data Tables **36**, 495 (1987).

20. I. Tanihata *et al.*, Phys. Lett. B **289**, 261 (1992).
21. I. Tanihata *et al.*, Phys. Lett. B **206**, 592 (1988).
22. J.S. Al-Khalili *et al.*, Phys. Rev. C **54**, 1843 (1996).
23. J.A. Tostevin *et al.*, Nucl. Phys. A **616**, 418c (1997).
24. W.R. Gibbs *et al.*, Phys. Rev. Lett. **67**, 1395 (1991).
25. J. Wurzer, Diploma thesis, University Erlangen (1994).
26. M. Tomaselli *et al.*, in *Proceedings of the International Conference on Nuclear Physics at the Borderlines, Lipary, Italy (2001)* (World Scientific, Singapore, 2002) p. 336, ISBN 981-02-4778-8.
27. I.J. Thompson *et al.*, Phys. Rev. C **49**, 1904 (1994).
28. H. Lenske *et al.*, Prog. Part. Nucl. Phys. **46**, 187 (2001).
29. O. Kisselev, F. Aksouh *et al.*, contribution to this volume.